Effect of bulk electric field reversal on the bounce resonance heating in dual-frequency capacitively coupled electronegative plasmas

Yong-Xin Liu,[1] Quan-Zhi Zhang,[1] Jia Liu,[1] Yuan-Hong Song,[1] Annemie Bogaerts,[2] and You-Nian Wang[1,a)]
[1]*School of Physics and Optoelectronic Technology, Dalian University of Technology, Dalian 116024, China*
[2]*Department of Chemistry, University of Antwerp, Campus Drie Eiken, Universiteitsplein 1, BE-2610 Wilrijk-Antwerp, Belgium*

(Received 7 August 2012; accepted 27 August 2012; published online 10 September 2012)

The electron bounce resonance heating (BRH) in dual-frequency capacitively coupled plasmas operated in oxygen and argon has been studied by different experimental methods. In comparison with the electropositive argon discharge, the BRH in an electronegative discharge occurs at larger electrode gaps. Kinetic particle simulations reveal that in the oxygen discharge, the bulk electric field becomes quite strong and is out of phase with the sheath field. Therefore, it retards the resonant electrons when traversing the bulk, resulting in a suppressed BRH. This effect becomes more pronounced at lower high-frequency power, when the discharge mode changes from electropositive to electronegative. © *2012 American Institute of Physics*. [http://dx.doi.org/10.1063/1.4751984]

Recently dual-frequency (DF) capacitively coupled plasmas (CCPs) have attracted increasing attention due to their interesting physics and particularly wide applications.[1] Electron heating by the time-varying fields is fundamental for the operation of various rf plasmas,[1–3] and the two typical heating mechanisms, i.e., Ohmic and stochastic heating, have been extensively studied over the past two decades.[2–6] In recent years, due to the growing industrial applications of rf discharges in the mTorr range, it becomes also increasingly important to understand the collisionless heating in rf discharges.[4–6]

The so-called "hard wall" model has been frequently employed as a paradigm to describe the collisionless heating. A phase randomization mechanism, which breaks the phase coherence between the electron motion and the electric field, is generally assumed, so that the electrons can gain net energy over a rf period.[2,3] Most earlier studies generally considered electron collisions with only one oscillating sheath. However, the so-called "double-sheath coherent heating," now generally called "bounce resonance heating (BRH)," has been elucidated in a particle-in-cell (PIC) Monte Carlo collision (MCC) simulation by Wood[7] for a CCP at low pressure (~3 mTorr). The BRH occurs in low pressure CCPs, when the driving frequency and electrode gap satisfy certain conditions, so that high-energy beamlike electrons created by one sheath expansion are bounced back and forth between two sheath edges, during which they can gain energy in each collision with either of the expanding sheaths, and consequently they can be heated by the two sheaths coherently. This BRH was later also studied by theories,[8,9] modeling,[10] and experiments.[11] However, in some cases,[10,11] the resonant electron energy is too small to affect the overall discharge. Recently, the BRH effect has been experimentally observed[12] in DF CCPs, and it was found to markedly enhance the discharge performance under certain conditions.

Generally, most studies of electron heating have focused on Ar discharges. However, in real applications, electronegative gases are most frequently employed. They are different from electropositive gas discharges in some basic, important features, such as the development of double layers,[13,14] a strong electric field and thus a high ionization rate in the bulk,[15] more pronounced modulation of the bulk electric field,[16,17] and a discharge mode transition induced by voltage or pressure.[18–20] These pronounced differences will have a substantial impact on the BRH, and the resultant electron energy probability function (EEPF) determines the basic discharge dynamics, such as dissociation, excitation, and ionization in electronegative discharges. Therefore, it is of fundamental importance to study the features of BRH in electronegative discharges.

In this letter, we investigate the BRH effects in a capacitive O_2 discharge with weak electronegativity ($= n_-/n_e < 12$) by a combination of different approaches: (i) a floating double probe to measure the positive ion density at the discharge center; (ii) a hairpin resonant probe to determine the electron density at the discharge center; (iii) an optical probe to detect the radially integrated light intensity at the center between both electrodes; and (iv) PIC MCC simulations to provide a description of the discharge dynamics and information about the spatiotemporal distribution of various plasma quantities. The combination of these approaches will elucidate the different behavior of BRH in electropositive and electronegative discharges.

Our experiments are performed in a parallel-plate DF (2/60 MHz) capacitive discharge chamber.[21] When conducting the optical measurements, the O_2 discharge is diluted with 5% Ar, as it is difficult to probe the emission from the direct excitation of molecule O_2. The measured electron density by the hairpin probe is corrected by using the fluid model described by Piejak.[22] In the experiment, we will compare the different behavior of BRH in Ar and O_2 and study the effect of high-frequency (HF) power on the BRH in the O_2 discharge.

Our simulations, which serve as a numerical explanation of the experiments of O_2 and Ar discharges, are based on the standard one-dimensional in space three-dimensional in

a)Electronic mail: ynwang@dlut.edu.cn.

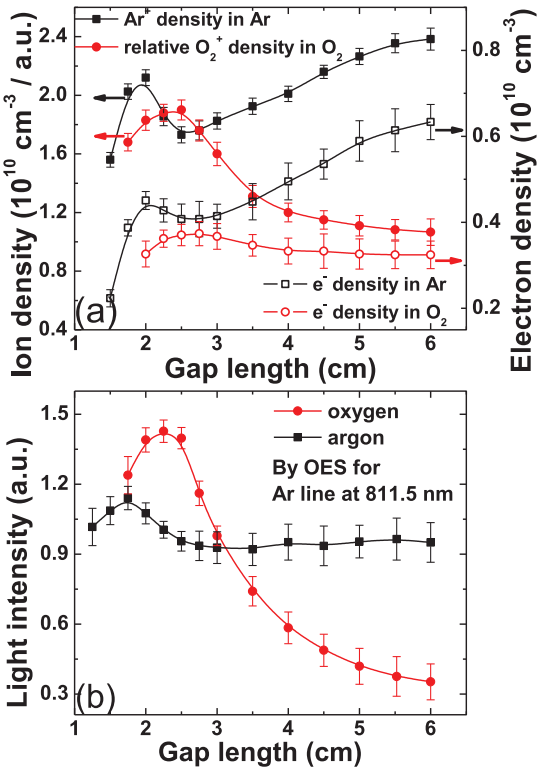

FIG. 1. Experimental measurements: positive ion and electron density (a) and light emission intensity (b) versus gap length, in Ar (black) and O_2 (red lines) discharges, at a fixed HF and LF power of 30 W and 100 W, respectively. All measurements are conducted at the center of the discharge gap. The light emission is detected for the Ar line at 811.5 nm and divided by the average intensity. Note that the pressure increases from 1.3 Pa in Ar to 4.0 Pa to sustain the O_2 discharge.

velocity (1D3V) electrostatic PIC MCC method. More details can be found in Ref. 21. To shed light on the BRH behavior at different HF powers in the experiments of O_2, we compare the spatiotemporal distribution of various plasma quantities (i.e., the electron impact ionization rate, bulk electric field, trajectory of a typical bouncing electron and its energy) for a range of HF voltages. In the case of the O_2 discharge, the charged particles O_2^+, O^-, and the electrons are traced using cross sections from Ref. 23. For Ar, the cross sections are the same as in Ref. 21.

Fig. 1 illustrates the measured positive ion density and electron density (a) as well as the emission intensity (b) versus gap length L, at a fixed HF and low-frequency (LF) power of 30 W and 100 W, for the Ar and O_2 discharge (black and red curves, respectively). The Ar^+ ion density is measured in absolute terms, whereas the O_2^+ density is only obtained in relative terms. The BRH effect is illustrated by the peak in ion and electron density and emission intensity at a certain gap length, called the resonant gap length. From this figure, the differences of the BRH effect between Ar and O_2 discharges can be generally summarized as followings.

(i) Compared with the Ar discharge, the most significant BRH effect in the O_2 discharge occurs at a somewhat larger gap, with the resonant peak broadened. The larger resonance gap and broader peak in the O_2 discharge is related to the electronegative discharge structure. In experiments, for instance, we observe an abnormal bright region, i.e., a double-layer structure, in the sheath region, as will be presented in a forthcoming paper.[24] In simulations, we observed a narrower bulk region and higher bulk electric field, as demonstrated below. The latter will influence the BRH in a subtle, but important manner, as explained below. Note that the position of the resonance peak is almost independent of the pressure in both Ar[21] and O_2.[24]

(ii) At $L > 2.5$ cm, the positive ion and electron densities drop monotonously in the O_2 discharge upon increasing L, while the plasma density rises in the Ar case. This is due to the more significant drop of the BRH with increasing L in the O_2 discharge, as can be observed from the light intensity curve in Fig. 1(b). It is worth to mention that our PIC MCC simulations have qualitatively reproduced the experimental density curves both in Ar and O_2.[24]

(iii) Comparing the O_2^+ ion and electron density in the O_2 discharge in Fig. 1(a), we can see that with decreasing L from 6 to 2.5 cm, the O_2^+ ion density increases by a factor of 1.8, while the electron density increases only by a factor of 1.1. Hence, at lower L, the electronegativity increases, which agrees qualitatively with the PIC MCC simulation (see below). This is attributed to the fact that for lower values of L, the electron dissociative attachment reaction $e + O_2 \rightarrow O + O^-$ is enhanced by the BRH, since this reaction has a considerable cross-section at $\varepsilon > 20$ eV, which lies well in the high-energy tail of the EEPF due to the BRH.

In order to understand better the underlying physics of the BRH effects, we analyze the different discharge structure in Ar and O_2 based on PIC MCC simulations. Fig. 2 illustrates the simulation results for 1.3 Pa in Ar (a) and 2.7 Pa in

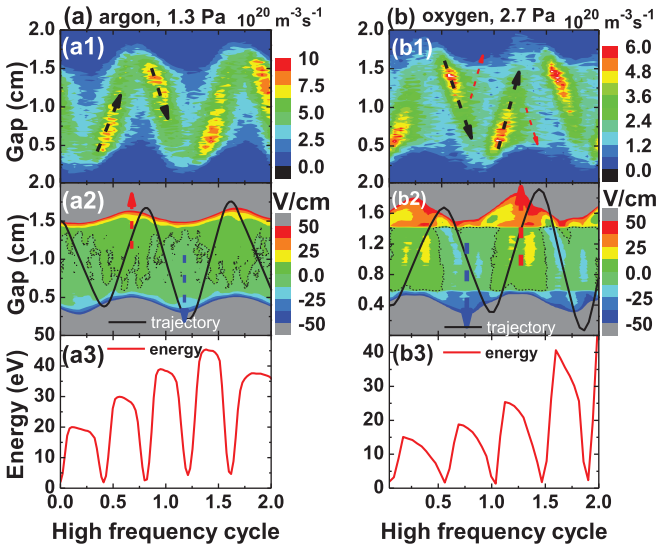

FIG. 2. PIC MCC simulation results obtained for 2 HF periods: spatiotemporal ionization rates ((a1) and (b1)), electric field inside the bulk and the trajectory (black solid line) of a typical bouncing electron ((a2) and (b2)), and its kinetic energy ((a3) and (b3)). The figures (a) and (b) correspond to Ar and O_2, respectively. The HF and LF voltage are 75 V, the electrode gap is 2 cm, and the pressure is 1.3 Pa in Ar and 2.7 Pa in O_2. Note that in figures (a2) and (b2), the thick blue and red dashed arrows indicate the direction of the electric field inside the bulk and the thin dashed black lines indicate the zero electric field contour line, to indicate where the bulk electric field changes direction.

the O_2 discharge (b) at fixed HF and LF voltages of 75 V and an electrode gap of 2 cm, during two HF cycles. The top figures (a1) and (b1) show the ionization rates, the middle figures (a2) and (b2) denote the bulk electric field and the typical trajectory of a bouncing electron (black curve), whose energy is plotted in the bottom figures (a3) and (b3). Comparing Fig. 2(a2) with Fig. 2(b2), we can see that the electric field in the bulk is stronger in O_2 ($\sim 10\,\mathrm{V/cm}$) and out of phase with the sheath field. This affects the BRH in two ways. On one hand, the low-energy electrons can obtain a substantial amount of energy from the high bulk electric field in O_2 so that their energy is beyond the minimum energy needed to join the BRH.[12,21] Some of these electrons may be assigned a large axial momentum by elastic collisions and collide with the sheath more efficiently. This enhances the BRH. On the other hand, and more importantly, the high-energy resonant electrons in O_2 will be retarded by the electric field reversal when traversing the bulk to the other electrode, resulting in a suppressed BRH, especially at strongly electronegative discharge conditions.

To elucidate the importance of the latter effect, we study the influence of the bulk electric field reversal on the high-energy bouncing electrons in detail. In Ar, we clearly see the electron beam bouncing between the two sheath edges, i.e., the BRH, from Fig. 2(a1) (marked by the black dashed arrow). In Figs. 2(a2) and 2(a3), one can see that a typical resonant electron sees a weak bulk electric field ($\sim 1\,\mathrm{V/cm}$) and its energy is almost constant when traversing the bulk. However, as seen in Fig. 2(a3), the electron clearly gains energy over 1 rf cycle.

In the electronegative O_2 discharge, on the other hand, the energetic beamlike electrons (marked by the black dashed arrow in Fig. 2(b1)) created by one-side sheath expansion are retarded and even repelled by a considerable bulk electric field reversal ($\sim$10 V/cm) (see Fig. 2(b2)) when penetrating into the plasma bulk. Hence, only the high-energy electrons can overcome this reversed bulk electric field and arrive at the opposite sheath at its expanding phase, where they obtain energy again so that BRH occurs. The repelled electrons, together with many other electrons that obtain energy only from the high bulk electric field, produce a visible ionization and their trails can be easily identified by the ionization zone (marked by the red dashed arrow in Fig. 2(b1)). However, the beamlike electrons, that suffer no collisions during their trajectory, arrive at the collapsing sheath and become decelerated. From Figs. 2(b2) and 2(b3), one can clearly see that a typical resonant electron always undergoes the reversal (retarding) electric field and loses its energy every time when traversing the bulk. In this sense, the BRH is suppressed by the bulk electric field in the electronegative discharge. However, since the bulk electric field is not strong enough, in general, the energy of a resonant electron still increases over 2 rf cycles.

The effect of HF power P_H on the BRH in the O_2 discharge is shown in Fig. 3, which displays the measured relative O_2^+ ion density and emission intensity versus L at different values of P_H with a fixed P_L of 100 W and a pressure of 4.0 Pa. At lower P_H, both the O_2^+ ion density and the plasma emission peaks gradually drop and almost disappear at $P_H = 20$ W, which indicates a suppressed BRH. It should

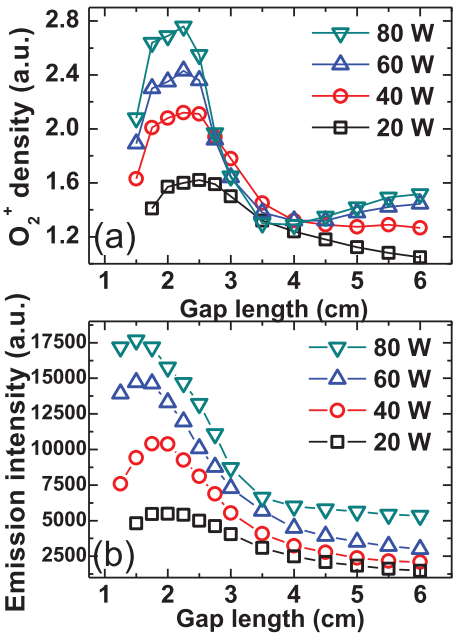

FIG. 3. Experimental measurements in the O_2 plasma: (a) relative O_2^+ ion density and (b) emission intensity (Ar line: 811.5 nm) at the discharge center versus L, at a range of HF powers P_H for a fixed LF power P_L of 100 W, at a gas pressure of 4.0 Pa. Note that the measured positive ion density has only relative values, because the ion Bohm velocity needs to be corrected according to the electronegativity in the sheath.

be noted that the results are quite different from the electropositive Ar discharge, where the BRH is hardly affected by P_H.[21] This is attributed to the fact that the O_2 discharge experiences a mode transition from electropositive to electronegative due to the lower amount of sheath heating with the drop of P_H. This mode transition induced by the driving voltage has been observed in CCPs with other electronegative gases as well.[18,19]

To reveal the different behavior of the BRH by changing the HF voltage V_H, we do again an analysis based on the PIC MCC simulations. In Fig. 4, simulation results are presented for the O_2 discharge in two HF cycles, at different values of V_H, i.e., 200 V, 75 V, and 50 V with a fixed V_L of 50 V, a gap of 2 cm, and a pressure of 4.0 Pa. By decreasing V_H from 200 V in Fig. 4(a) to 50 V in Fig. 4(c), our simulations predict that the discharge experiences a mode transition from electropositive ($\alpha = 0.3$) to electronegative ($\alpha = 11$). In the electropositive discharge (Fig. 4(a)), at a resonance gap of 2 cm, we see that the high-energy beamlike electrons (marked by the black dashed arrow) are bounced back and forth between the two sheath edges. From Figs. 4(a2) and 4(a3), one can see that a typical resonant electron sees a weak bulk electric field ($\sim$1 V/cm) when traversing the bulk, similar to the Ar discharge in Fig. 2(a). With decreasing V_H, the O_2 discharge becomes more electronegative, and consequently the electric field in the bulk increases ($\sim$10 V/cm; see Fig. 4(b2)). As V_H drops further to 50 V, the electronegativity and the electric field in the bulk increase further (up to 15 V/cm; see Fig. 4(c2)), and in this case, even the much higher energy electrons can be repelled by the electric field when traversing the bulk to the other electrode, as shown in Fig. 4(c1), hence the BRH is greatly suppressed. In other words, the high electric field reversal inside the bulk

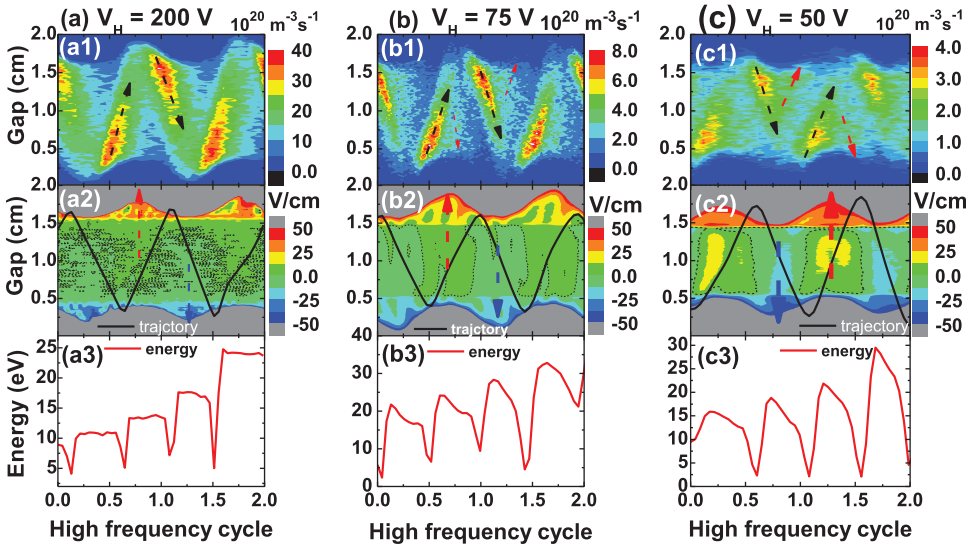

FIG. 4. PIC MCC simulation results obtained for 2 HF periods in the O_2 plasma at $V_H = 200$ V (a), 75 V (b), and 50 V (c): spatiotemporal ionization rates ((a1), (b1), and (c1)), electric field inside the bulk and the trajectory (black solid line) of a typical bouncing electron ((a2), (b2), and (c2)), and its energy ((a3), (b3), and (c3)). The electrode gap is 2 cm, the LF voltage is 50 V, and the pressure is 4.0 Pa. Note that in figure (a2), (b2), and (c2), the thick blue and red dashed arrows indicate the direction of the electric field inside the bulk and the thin dashed black lines indicate the zero electric field contour line.

decelerates these electrons bouncing between two expanding sheath edges and consequently suppresses the BRH, which explains the drop of the O_2^+ ion density and emission intensity at the resonance gap when P_H decreases in the experiments shown in Fig. 3.

In particular, when the bulk electric field is strong enough, the electron energy loss to the reversal electric field can become comparable or even larger than the energy gained from the expanding sheath, so that the BRH cannot happen. This situation will be more common in more strongly electronegative discharges, such as, CF_4 and SF_6, where the bulk electric field reaches values up to 40 V/cm.[18]

In conclusion, we investigated the different behavior of collisionless electron BRH in low-pressure DF electropositive and electronegative CCPs. In comparison with the electropositive Ar discharge, the BRH in the electronegative O_2 discharge occurs at a larger electrode gap. This is related to the O_2 discharge structure, i.e., the development of a double layer in the sheath, the narrower bulk region and higher electric field reversal in the bulk. PIC MCC simulation indeed shows that in the O_2 discharge, the bulk electric field reversal becomes quite strong and is out of phase with the sheath field, hence retarding the resonant electrons when traversing the bulk, resulting in a suppressed BRH. This was further confirmed experimentally in the O_2 discharge by the fact that with lower HF power, the resonance peaks in positive ion density and emission intensity drop. This is attributed to the enhancement of the electric field reversal in the bulk when the discharge shifts from electropositive to electronegative mode with the drop of HF power. This electric field structure is not exclusive for O_2. It is a general property for electronegative discharges operating in a higher frequency (~60 MHz). O_2 is classified as a weak electronegative gas, so the rf discharge structure may differ from strongly electronegative gases, such as, CF_4 and SF_6, where we expect different features of the BRH.

This work was supported by the Important National Science and Technology Specific Project (Grant No. 2011ZX02403-001), the Fundamental Research Funds for the Central Universities (Grant No. DUT11ZD109), the International Science & Technology Cooperation Program of China (Grant No. 2012DFG02150), and the joint research project in the framework of the agreement between MOST and FWO.

[1]M. A. Lieberman and A. J. Lichtenberg, *Principles of Plasma Discharges and Materials Processing* (Wiley, New York, 2005).
[2]M. A. Lieberman and V. A. Godyak, IEEE Trans. Plasma Sci. **26**, 955 (1998).
[3]M. M. Turner, J. Phys. D: Appl. Phys. **42**, 194008 (2009).
[4]M. Surendra, D. B. Graves, and I. J. Morey, Appl. Phys. Lett. **56**, 1022 (1990).
[5]M. Surendra and D. Vender, Appl. Phys. Lett. **65**, 153 (1994).
[6]Y. Okuno, Y. Ohtsu, and H. Fujita, Appl. Phys. Lett. **64**, 1623 (1994).
[7]B. P. Wood, Ph.D. dissertation, University of California, Berkeley, 1991.
[8]Y. M. Aliev, I. D. Kaganovich, and H. Schlüter, Phys. Plasmas **4**, 2413 (1997).
[9]I. D. Kaganovich, V. I. Kolobov, and L. D. Tsendin, Appl. Phys. Lett. **69**, 3818 (1996).
[10]G. Y. Park, S. J. You, F. Iza, and J. K. Lee, Phys. Rev. Lett. **98**, 085003 (2007).
[11]S. J. You, C. W. Chung, and H. Y. Chang, Appl. Phys. Lett. **87**, 041501 (2005).
[12]Y. X. Liu, Q. Z. Zhang, W. Jiang, L. J. Hou, X. Z. Jiang, W. Q. Lu, and Y. N. Wang, Phys. Rev. Lett. **107**, 055002 (2011).
[13]N. Nakano, N. Shimura, Z.-L. Petrović, and T. Makabe, Phys. Rev. E **49**, 4455 (1994).
[14]V. A. Lisovskiy and V. D. Yegorenkov, Vacuum **80**, 458 (2006).
[15]M. Shibata, N. Nakano, and T. Makabe, J. Appl. Phys. **77**, 6181 (1995).
[16]M. Yan, A. Bogaerts, W. J. Goedheer, and R. Gijbels, Plasma Sources Sci. Technol. **9**, 583 (2000).
[17]M. Yan, A. Bogaerts, and R. Gijbels, J. Appl. Phys. **87**, 3628 (2000).
[18]J. Schulze, A. Derzsi, K. Dittmann, T. Hemke, J. Meichsner, and Z. Donkó, Phys. Rev. Lett. **107**, 275001 (2011).
[19]O. V. Proshina, T. V. Rakhimova, A. T. Rakhimov, and D. G. Voloshin, Plasma Sources Sci. Technol. **19**, 065013 (2010).
[20]K. Denpoh and K. Nanbu, Jpn. J. Appl. Phys., Part 1 **39**, 2804 (2000).
[21]Y. X. Liu, Q. Z. Zhang, W. Jiang, W. Q. Lu, and Y. N. Wang, Plasma Sources Sci. Technol. **21**, 035010 (2012).
[22]R. B. Piejak, V. A. Godyak, R. Garner, B. M. Alexandrovich, and N. Sternberg, J. Appl. Phys. **95**, 3785 (2004).
[23]V. Vahedi and M. Surendra, Comput. Phys. Commun. **87**, 179 (1995).
[24]Y. X. Liu, Q. Z. Zhang, A. Bogaerts, and Y. N. Wang, "The bounce resonance heating in a dual-frequency capacitively coupled electronegative oxygen discharge" (unpublished).